ISSN (Print) 1226-1750
ISSN (Online) 2233-6656
Journal of Magnetics 18(3), 255-259 (2013) http://dx.doi.org/10.4283/JMAG.2013.18.3.255

Numerical Analysis for Characterization of Single Phase Induction Motors by using Circuit Equations Coupled with Magnetic Field Distribution

Young Sun Kim and Dong Yoon Lee*

Department of Electrical and Electronic Engineering, Joongbu University, Geumsan 302-702, Korea

(Received 22 January 2013, Received in final form 27 June 2013, Accepted 1 July 2013)

In this paper a new coupling method for efficient and simple analysis of single phase induction motor is presented. The circuit representation of both the stator winding and each conducting rotor loop (composed of rotor bar and end ring segment) is used in conjunction with the distribution of magnetic flux linkage instead of inductance matrix. The flux linkage is calculated using air-gap flux density distributions driven by unit currents in the stator windings and rotor bars. The field distribution of one turn of a coil is calculated by FEM and the result is used to calculate total flux linkage by employing a coordinate transformation. The numerical results give good agreement with prior literature. The method is particularly effective in analyzing the effect of the number of rotor bars.

Keywords : single phase induction motor, travelling wave, finite element method, coupling method

Introduction

Single phase induction motors are used in applications with power requirements of less than 1 kW even with a lower efficiency and higher cost than a multiphase induction motor of the same power specifications. The reason for this is the convenient availability of the single phase power supply. As a result, this motor does not have a rotating magnetic field like its three-phase counterpart. The magnetic field of a single phase induction motor operates by adjusting the field magnitude while maintaining its direction, also known as a standing wave. The resulting starting torque does not generated in initial driving stage because the magnetic field by the stator winding does not rotate [1-3]. However, once the rotor begins to move then the motor generates an induced torque to keep driving.

There are two main theories in the classical theory for the operating characteristics of a single phase induction motor: the two-motor theory of two rotating fields and the cross field theory [4]. However, both theories can not accurately describe the coil distribution and magnetic field distribution and as a result, effects of the number of rotor bars is not characterized [5]. On the other hand, a full finite element analysis requires massive calculation time and complex modeling techniques for time-stepping eddy current problem and remeshing.

In this paper, the circuit concept is applied to the stator winding and the rotor conductor loops composed of rotor bar and end ring segment. The flux linkages obtained from FE field analysis are employed instead of inductance matrix [6]. The flux linkage is calculated using the air gap field distribution by a unit current in stator and rotor bars. The total flux linkage of external circuit equation is easily calculated using superposition of each coil field and a coordinate transformation. As a result, this method requires only few field analyses of a unit current of stator and rotor conductor. Once the flux parameters are obtained, the overall motor characteristics such as stator current, rotor bar current, torque are easily calculated in both transient state and steady state [7-10]. The transient characteristics of all the currents are calculated in a recursive form by using finite time difference scheme.

2. Coupling Algorithm of Circuit and Magnetic Field

2.1. Flux Distribution Patterns

Considering cylinder symmetry, flux distribution pattern by stator winding, and rotor bar currents are shown in

*Corresponding author: Tel: +82-41-750- 6209
Fax: +82-41-750-6402, e-mail: dylee@joongbu.ac.kr

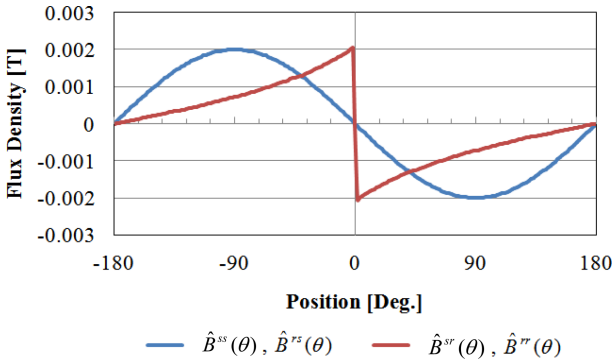

Fig. 1. (Color online) Air-gap flux distribution by stator winding and single rotor bar current.

Fig. 1. Flux distribution by stator winding current is assumed to be sinusoidal distributed at the fundamental frequency only. There are several assumptions in this process for the qualitative analysis of the motor. The main consideration is that the motor has very small air gap and no slot effect.

Here each of the sources is driven with a unit current and the magnetic flux density is calculated using FEM techniques along the surface of the rotor and the interior side of the stator respectively. Nomenclatures for flux density in Fig. 1 are drawn below figure.

2.2. Stator Circuit Equation

The circuit equation of a stator winding which has a single turn is represented as (1)

$$V(t) = R^s\, i^s(t) + \frac{d}{dt}\int B^s(\theta,t)\, ds \tag{1}$$

where $V(t)$ is applied voltage for one turn, R^s is resistance of stator winding, $i^s(t)$ is stator winding current, $B^s(\theta, t)$ is stator flux density, it is resultant flux density made by stator winding current $i^s(t)$ and rotor bar currents $i_j^r(t)$ as in (2)

$$B^s(\theta,t) = \hat{B}^{ss}(\theta)\, i^s(t) + \sum_{j=1}^{n_b} \hat{B}_j^{sr}(\theta)\, i_j^r(t) \tag{2}$$

where n_b is the number of rotor bars, $\hat{B}_j^{ss}(\theta)$ is the flux density by stator winding driven with a unit current, $\hat{B}_j^{ss}(\theta)$ denotes the flux density by rotor bar driven with a unit current.

For N turns of stator winding the circuit equation can be written as (3).

$$\begin{aligned} & NR^s\, i^s(t) \;+\; N^2 \int \hat{B}^{ss}(\theta)\, ds \frac{d}{dt} i^s(t) \\ & +\; N\sum_{j=1}^{n_b} \int \hat{B}_j^{sr}(\theta)\, ds \frac{d}{dt} i_j^r(t) \;=\; V(t) \end{aligned} \tag{3}$$

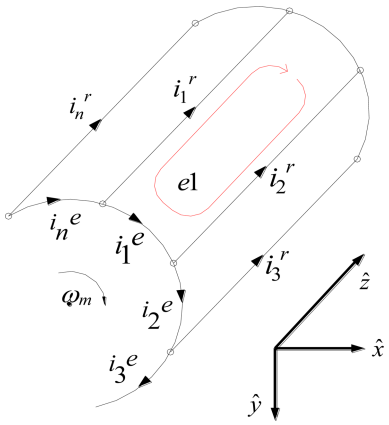

Fig. 2. (Color online) Loop circuits of the rotor.

2.3. Rotor Circuit Equations

Fig. 2 shows the rotor circuit of a single phase induction motor. In the figure, i_j^r, i_j^e, ω and i_j^e (j = 1, 2, 3 …) stand for bar currents, end-ring currents, rotor speed and EMFs induced in each single loop, respectively.

In Fig. 2 the EMF of the j-th loop is induced by the time variation of flux linkage and is equal to the sum of voltage drops across that loop.

$$\frac{d}{dt}\int_j B^r(\theta,t)\, ds = r_b(i_j^r - i_{j+1}^r) - 2r_e\, i_j^e \tag{4}$$

Where, $B^r(\theta, t)$ is the magnetic flux density distribution along the rotor surface, r_b resistance of rotor bar and r_e resistance of end-ring located between bars. $B^r(\theta, t)$ in (4) can be written as (5).

$$B^r(\theta,t) = N\,\hat{B}^{rs}(\theta)\, i^s(t) + \sum_{j=1}^{n_b} \hat{B}_j^{rr}(\theta)\, i_j^r(t) \tag{5}$$

Substituting (5) into (4), the differential equations for currents can be obtained as (6).

$$\begin{aligned} & Nl\int \hat{B}^{rs}(\theta)\, d\theta \frac{d}{dt} i^s(t) + l\int \sum_{j=1}^{n_b} \hat{B}_j^{rr}(\theta)\, d\theta \frac{d}{dt} i_j^r(t) \\ & = r_b(i_j^r(t) - i_{j+1}^r(t)) - 2r_e\, i_j^e(t) \end{aligned} \tag{6}$$

Where, l is the axial length of rotor bar, and the currents i_j^r and i_j^e satisfy the Kirchhoff's current law at the connection nodes between the rotor bars and end-rings.

$$\{i^r\} + [D]^T \{i^e\} = \{0\} \tag{7}$$

Where $[D]^T$ is the matrix for the relationship between the currents of the rotor bars and end-rings.

After combining differential equations (1), (4) and (7), and applying the time difference method, the final recursive relation between the currents can be obtained in matrix form.

$$\left(\frac{1}{\Delta t}\begin{bmatrix} A_{ss} & \mathbf{A}_{sr} & \mathbf{0} \\ \mathbf{A}_{rs} & \mathbf{A}_{rr} & \mathbf{0} \\ \mathbf{0} & \mathbf{0} & \mathbf{0} \end{bmatrix} + \begin{bmatrix} B_{ss} & 0 & \mathbf{0} \\ 0 & \mathbf{B}_{rr} & \mathbf{B}_{re} \\ \mathbf{0} & \mathbf{B}_{er} & \mathbf{B}_{ee} \end{bmatrix}\right)^{t+\Delta t} \begin{Bmatrix} i^s \\ \mathbf{i}^r \\ \mathbf{i}^e \end{Bmatrix}^{t+\Delta t} = \frac{1}{\Delta t}\begin{bmatrix} A_{ss} & \mathbf{A}_{sr} & \mathbf{0} \\ \mathbf{A}_{rs} & \mathbf{A}_{rr} & \mathbf{0} \\ \mathbf{0} & \mathbf{0} & \mathbf{0} \end{bmatrix}^{t} \begin{Bmatrix} i^s \\ \mathbf{i}^r \\ \mathbf{i}^e \end{Bmatrix}^{t} + \begin{Bmatrix} V \\ \mathbf{0} \\ \mathbf{0} \end{Bmatrix}^{t+\Delta t} \tag{8}$$

where

$$\Delta t = \frac{\Delta\theta}{\omega}$$

$$A_{ss} \quad : N^2 l \sum_{i=1}^{ns} \sum_{j=1}^{2ns} \int \hat{B}_j^{\,ss}(\theta)\, d\theta$$

$$B_{ss} \quad : NR^s$$

$$[\mathbf{A}_{sr}]_{1j} \quad : Nl \sum_{i=1}^{ns} \sum_{j=1}^{nb} \int \hat{B}_j^{\,sr}(\theta)\, d\theta$$

$$[\mathbf{A}_{rs}]_{i1} \quad : Nl \sum_{i=1}^{ns} \sum_{j=1}^{2ns} \int \hat{B}_j^{\,rs}(\theta)\, d\theta$$

$$[\mathbf{A}_{rr}]_{ij} \quad : l \sum_{i=1}^{nb} \sum_{j=1}^{nb} \int \hat{B}_j^{\,rr}(\theta)\, d\theta$$

$$[\mathbf{B}_{rr}]_{ij} \quad : \sum_{i=1}^{nb} \sum_{j=1}^{nb} (-r_b)_{i=j} \text{ and } (r_b)_{j=i+1}$$

$$[\mathbf{B}_{re}]_{ij} \quad : \sum_{i=1}^{nb} \sum_{j=1}^{nb} (2r_e)_{i=j}$$

$$[\mathbf{B}_{er}]_{ij} \quad : \sum_{i=1}^{nb} \sum_{j=1}^{nb} (1)_{i=j}$$

$$[\mathbf{B}_{ee}]_{ij} \quad : [D]^T$$

In above (8), the unknown variables are the sum of the stator current, the number of rotor bar current and the end-ring current. With the structure of rotor bars, speed and applied voltage, all the currents flowing the stator coil, rotor bars and end-rings of single phase induction motors can be calculated by using (8).

2.4. Torque Equation

The produced torque T of the specified motor can also be calculated with the resultant currents from (8) and magnetic flux density distribution patterns. Using the Lorentz force equation gives the following equation.

$$T = \sum_{j=1}^{n_b} r_j\, B_j^{\,r}(\theta, t)\, i_j^{\,r}\, l \tag{9}$$

where r_j denotes the radius of the rotor.

3. Numerical Applications

Fig. 3 shows cross sectional view of a 2-pole single phase induction motor. The stator coils consist of two coil sides and the rotor bars are located at equal distance. P1, P2 and P3 are the test points for magnetic flux pattern to know the wave characteristics of the rotating magnetic field.

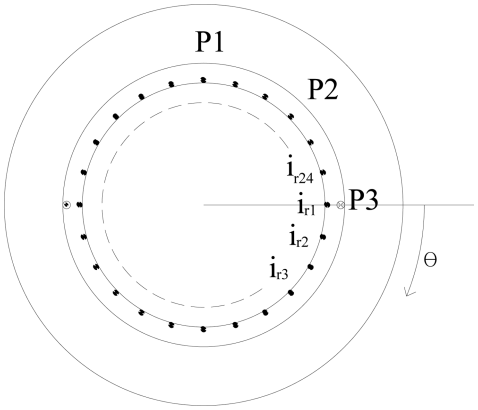

Fig. 3. Cross section of analysis model.

The voltage and the frequency of the power source is applied to the analysis model (Fig. 3) in specific slip of S = 0.05. And the system equation is solved iteratively until the motor reaches steady state. The applied voltage and primary current waveforms are shown in Fig. 4 while the

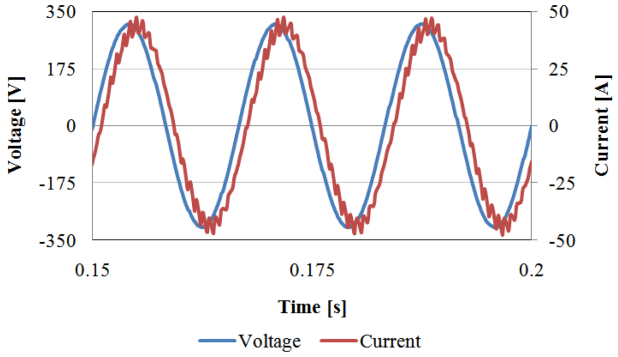

Fig. 4. (Color online) Input voltage and winding current waveform of stator.

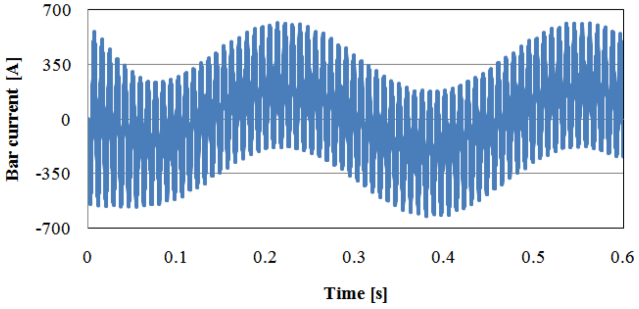

Fig. 5. (Color online) Rotor bar current waveform that has group frequency.

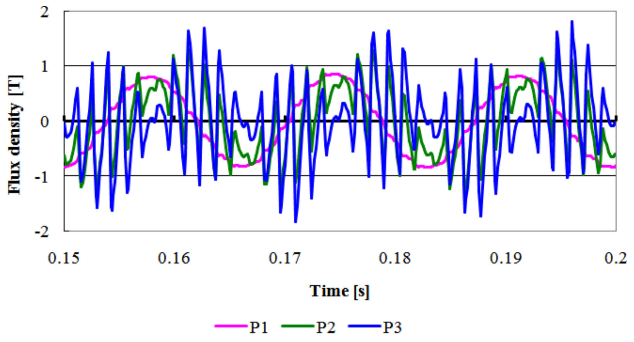

(a) Slip: 0.5

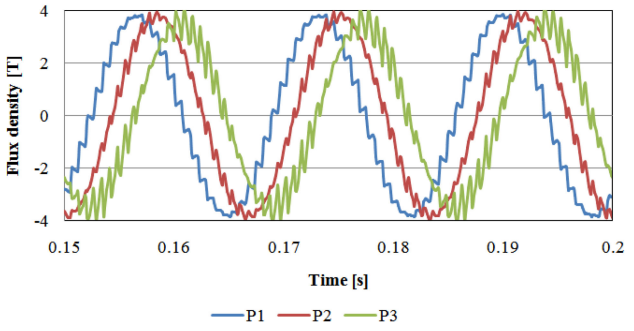

(b) Slip: 0.05

Fig. 6. (Color online) Flux density patterns at several fixed points.

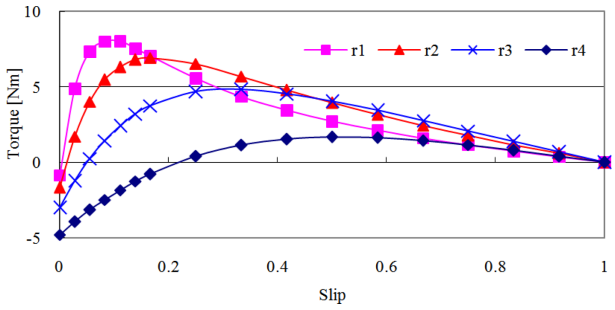

Fig. 7. (Color online) Characteristic of average torque and speed.

Fig. 5 shows the current pattern of a rotor bar with group frequency which depends on motor speed. The magnetic flux patterns at points P1, P2 and P3 are drawn in Fig. 6(a) and Fig. 6(b) for different motor speed. In Fig. 6, the fields travel just like in multiphase machines while the motor is rotating. Therefore, it might say that the magnetic field variation(travelling wave) of the motor is the rotating magnetic field.

Fig. 7 presents torque-speed characteristics for the several resistances of rotor circuits, where the resistances are $r_1 < r_2 < r_3 < r_4$. In Fig. 7, the bigger secondary resistance produces the less maximum torque and even

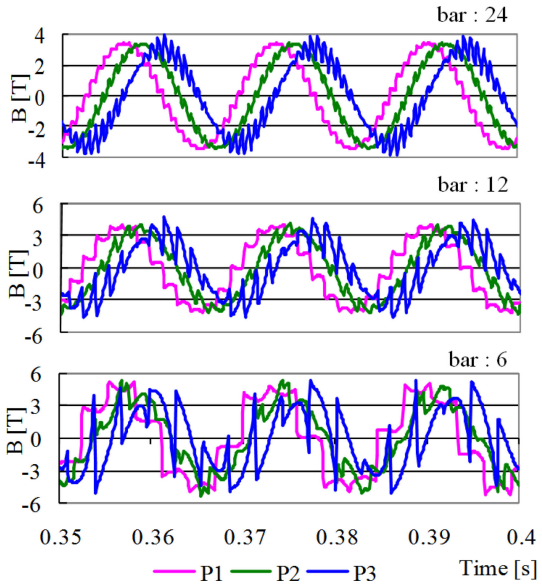

Fig. 8. (Color online) Magnetic flux density patterns for the variation of the number of bars at several fixed points.

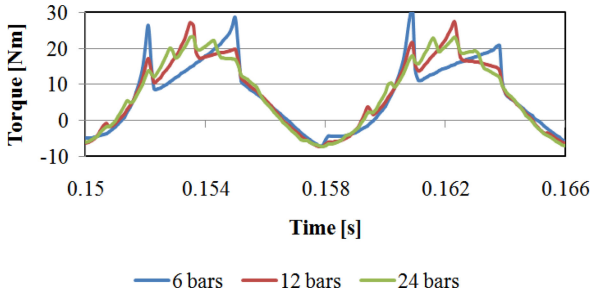

Fig. 9. (Color online) Torque pulsation by number variation of the rotor bar.

negative torque through wider range in slip.

The effect of the number of rotor bars, (8) is solved for the cases of 6, 12 and 24 rotor bars. In each case, the total cross sectional area, applied voltage, and slip are held constant. The flux patterns for the variation of the number of bars and the torque are shown in Fig. 8 and Fig. 9. These patterns clearly indicate that as the number of bars of a motor increases the higher harmonics in the waveforms are decreased.

4. Conclusion

A new analysis method is demonstrated in this paper to model the effect of the number of rotor bars. In this method, circuit theory concepts are applied to stator winding and each loop of rotor composed of rotor bar and end-ring segment and flux linkage concepts are used instead of inductance matrix.

As a result, this method agrees with the existing theory

in steady state characteristics and accordingly is very effective in demonstrating the effect of the number variation of rotor bars. In addition, the voltage-current characteristics of the stator winding and the eddy currents for rotor bars are shown. The magnetic field in the motor driven by a single phase source are also analyzed illustrating whether the field is rotating or not. Increasing the number of rotor bars in the motor decreases the higher order harmonics in the generated torque and magnetic field distribution. Further studies about characteristics with slots and nonlinear effect of iron core should be investigated.

Acknowldgment

This research was supported by Basic Science Research Program through the National Research Foundation of Korea (NRF) funded by the Ministry of Education, Science and Technology (2012R1A1A1040410).

References

[1] Austin Hughees, and Bill Drury, Electric motors and drives: fundamentals, types and applications, 3rd Ed., Newnes, Burlington (2006).
[2] Charles F. Holmes, Design of a single-phase induction motor, Ulan Press (2012).
[3] Bahram Amin, Induction motor: Analysis and torque control, Springer, Berlin, New York (2002).
[4] Gyril G. Veninott, E. E., D. Eng. Theory and design of small induction motors, McGraw Hill (1959).
[5] N. Sadowski, R. Carlson, S. R. Arruda, C. A. da Silva, and M. Lajoic-Mazenc, IEEE Trans. Magn. **31**, 1908 (1995).
[6] Sheppard J. Salon, Finite element analysis of electrical machines, Kluwer Academic Publisher, New York (1995).
[7] Katsumi Yamazaki, IEEE Trans. Magn. **38**, 1281 (2002).
[8] De Gersem, H. and Hameyer, K., IEEE Trans. Magn. **38**, 1221 (2002).
[9] Xiuhe Wang, Changqing Zhu, Rong Zhang, Renyuan Tang, and Hahn Song-Yop, IEEE Trans. Magn. **42**, 587 (2006).
[10] Ningze Tong, Fengge Zhang, and Jianwei Wang, ICEMS 2008, 4127 (2008).